SKO rat develops impairment of spatial working memory

We evaluated the spatial working memory by Y-maze test for the assessment of mental development in SKO rats. Y-maze score was significantly lower in SKO rats than that in WT rats (Fig. 3A) while spontaneous movement was unchanged. To determine whether this impairment of spatial working memory is seipin knockout specific, we performed the same experiment in leptin-deficient Lep^{mkyo}/Lep^{mkyo} rats and A-ZIP/F-1 mice, a mouse model of generalized lipodystrophy due to adipocyte specific expression of dominant negative protein for b-zip protein (22). Both Lep^{mkyo}/Lep^{mkyo} rats and A-ZIP/F-1 mice showed no significant change in Y-maze score when compared with their WT littermates, respectively, indicating that the impairment of spatial working memory in SKO rats is due to neither leptin deficiency nor lipodystrophy (Fig. 3B and C).

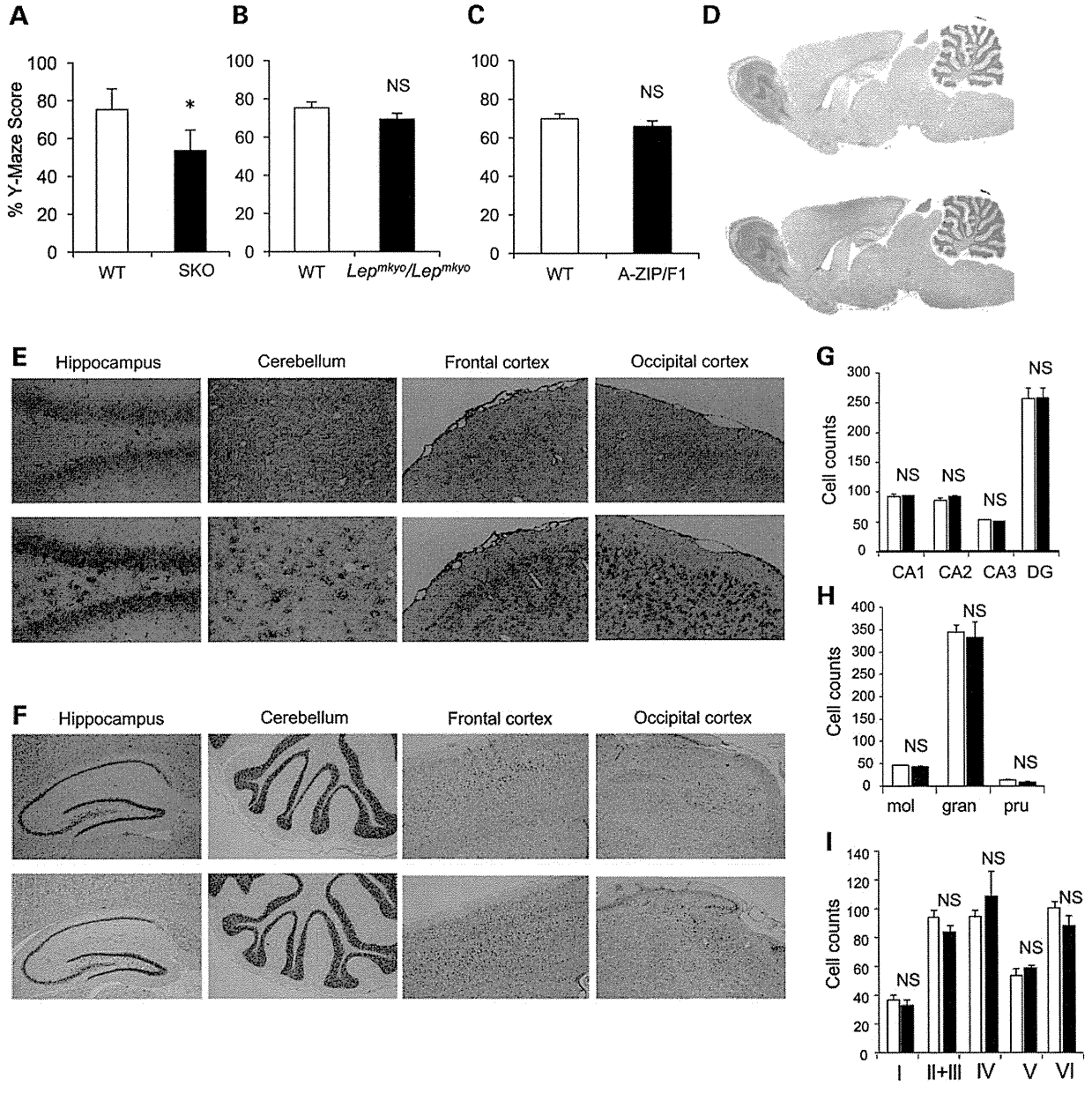

Figure 3. The role of seipin in the brain development. (A–C) Y-maze score as an index of spatial working memory in SKO rats (A), Lep^{mkyo}/Lep^{mkyo} rats (B) and A-ZIP/F-1 mice (C). Values are mean ± SEM ($n = 10$ per group). *$P < 0.05$, NS, not significant (Student's *t*-test). (D and E) Bscl2 expression pattern in the whole brain (D) and sections (E) of hippocampus, cerebellum, frontal cortex and occipital cortex assessed by *in situ* hybridization in a WT rat. Images used with sense probe (top) and antisense probe (bottom) are shown. Original magnification of ×16 is shown for the whole brain. ×200 is for hippocampus and cerebellum and ×100 is for frontal and occipital cortexes. (F) Microscopic images of hippocampus, cerebellum, frontal cortex and occipital cortex in WT (top) and SKO rats (bottom). Nissl staining was used. Original magnification of ×40 is shown. (G–I) The number of Nissl stained cells in four regions (CA1, CA2, CA3, DG) of hippocampus (G), five layers (I, II+III, IX, V, VI) of frontal cortex (H) and three layers (molecular cell layer, granular cell layer and Purkinje cell layer) of cerebellum (I) in SKO rats (closed bars) and their WT littermates (open bars). Values are means ± SEM ($n = 9$ per group). NS, not significant (Student's *t*-test).

The role of seipin in the brain development

Gene expression pattern of *Bscl2* in the whole brain was analyzed by *in situ* hybridization in WT rats. *Bscl2* gene was ubiquitously expressed throughout the brain including hippocampus, cerebellum and, frontal and occipital cortex in WT rats (Fig. 3D and E). Next, we histologically examined of the brain in SKO rats. In comparison with WT rats, any morphological changes were not detected throughout the brain in SKO rats (Fig. 3F). Since the whole brain weight was slightly but significantly decreased in SKO rats (Fig. 1F), we examined the neuron density in hippocampus, cerebellum and frontal cortex. In any layers or regions of these sections, no significant change of neuron density was detected (Fig. 3G–I). The fact that the brain volume was decreased while neuron density was unchanged means that the total neuron number in the brain was decreased.

Intellectual quotient test and brain volume in human BSCL2 patient

Intellectual quotient test was examined in two male and four female BSCL2 patients. The age of these six patients was ranging from 18 to 36 years (Supplementary Material, Table. S1). Four patients had R275X, one patient had E189X and the remaining one had Y187C homozygous mutation in *BSCL2* gene, respectively. Five of six patients showed mild but obvious reduction in both verbal and performance intelligence quotient scores. Brains of the same six patients were examined by MRI. No apparent morphological change was reported with these MRI examinations in any patients. For the analysis of brain volume, three male and six female healthy subjects whose age was ranging from 21 to 34 years (mean, 25.4 years) with normal body mass index between 18.5 and 25.0 kg/m^2 were also examined by MRI. With the small number of subjects, we found no significant difference but the tendency of reduction in whole brain volume in the patients when compared with healthy subjects (Fig. 4A). Next, we checked the brain parenchymal area of coronal sections at three different levels. In two of the three sections, significant reduction of brain parenchymal area was observed in the patients (Fig. 4B). Finally, we checked the brain parenchymal /subarachnoid area ratio to assess the presence of brain atrophy. No significant difference of this ratio was observed at any levels between the patients and healthy subjects, indicating that the reduction of brain volume in BSCL2 patients was not due to brain atrophy (Fig. 4C).

Male SKO rat shows infertility with azoospermia

Although serum levels of hormones including lutenizing hormone (LH), follicle stimulation hormone (FSH) and testosterone, in male SKO rats were all within normal range and showed no significant difference from those in male WT rats (Supplementary Material, Fig. S7), male SKO rats showed remarkably small testis in weight when compared with WT rats (Fig. 5A and D) and were infertile while female SKO rats were fertile. There was no significant change in testis weight in both Lep^{mkyo}/Lep^{mkyo} rats and A-ZIP/F-1 mice when compared with that in their WT littermates, respectively (Fig. 5B–E). Testis histology showed markedly shrunk spermatic duct and lack of mature sperm cells in SKO rats while there was no change in both Lep^{mkyo}/Lep^{mkyo} rats and A-ZIP/F-1 mice when compared with their WT littermates (Fig. 5D and E). These results indicate that azoospermia in SKO rats is due to neither leptin deficiency nor lipodystrophy.

The role of seipin in the spermatogenesis

Gene expression of *Bscl2* in testis was analyzed with two infertile mouse models. One was Sl/Sl^d mutant mouse that has Sertoli cell dysfunction and the other was W/W^v mutant mouse that has lack of functional C-Kit (23,24). *Bscl2* gene expression was detected in WT mice but not in Sl/Sl^d and W/W^v mice, indicating that *Bscl2* gene is expressed in neither Sertoli nor Spermatogonia cells (Fig. 5F). Gene expression of *Bscl2* during the period of postnatal development in WT rat testis was examined and the significant increment was detected from 5 to 6 weeks (Fig. 5G). Most rats reach sexual maturity at 6 or 7 weeks old. Finally, gene expression pattern of *Bscl2* in testis was analyzed by *in situ* hybridization in WT rats (Fig. 5H). *Bscl2* gene was expressed in spermatocytes and mature sperm cells but not in spermatogonia cells. These results indicate that seipin might have an important role especially in the late phase of spermatogenesis.

Semen examination and gonadal hormone concentrations in human BSCL2 patients

Semen and gonadal hormone concentrations were examined in two male patients with BSCL2. On semen examination, one patient showed obvious oligospermia and the other patient showed normal but minimum of the normal range value in all parameters (Table 1). On the other hand, gonadal hormone

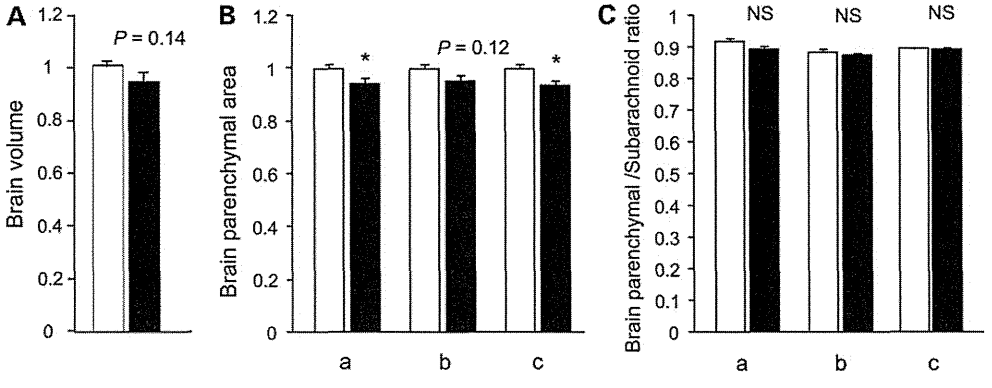

Figure 4. MRI analysis of brain volume in human BSCL2 patients. (A) Whole brain volume in BSCL2 patients (closed bar) and healthy subjects (open bar). The fold change was displayed as relative to healthy subjects. (B) Brain parenchyma area of coronal sections at three different levels in BSCL2 patients (closed bar) and healthy subjects (open bar). (C) Brain parenchyma/subarachnoid area ratio at three different levels in BSCL2 patients (closed bar) and healthy subjects (open bar). Three different levels: (a) the level just above the bilateral ventricles, (b) the level in the center of the lateral ventricles, (c) the level through interventricular foramen. Values are mean ± SEM (Healthy subjects; $n = 9$, BSCL2 patients; $n = 6$). *$P < 0.05$, **$P < 0.01$, NS, not significant (Student's t-test).

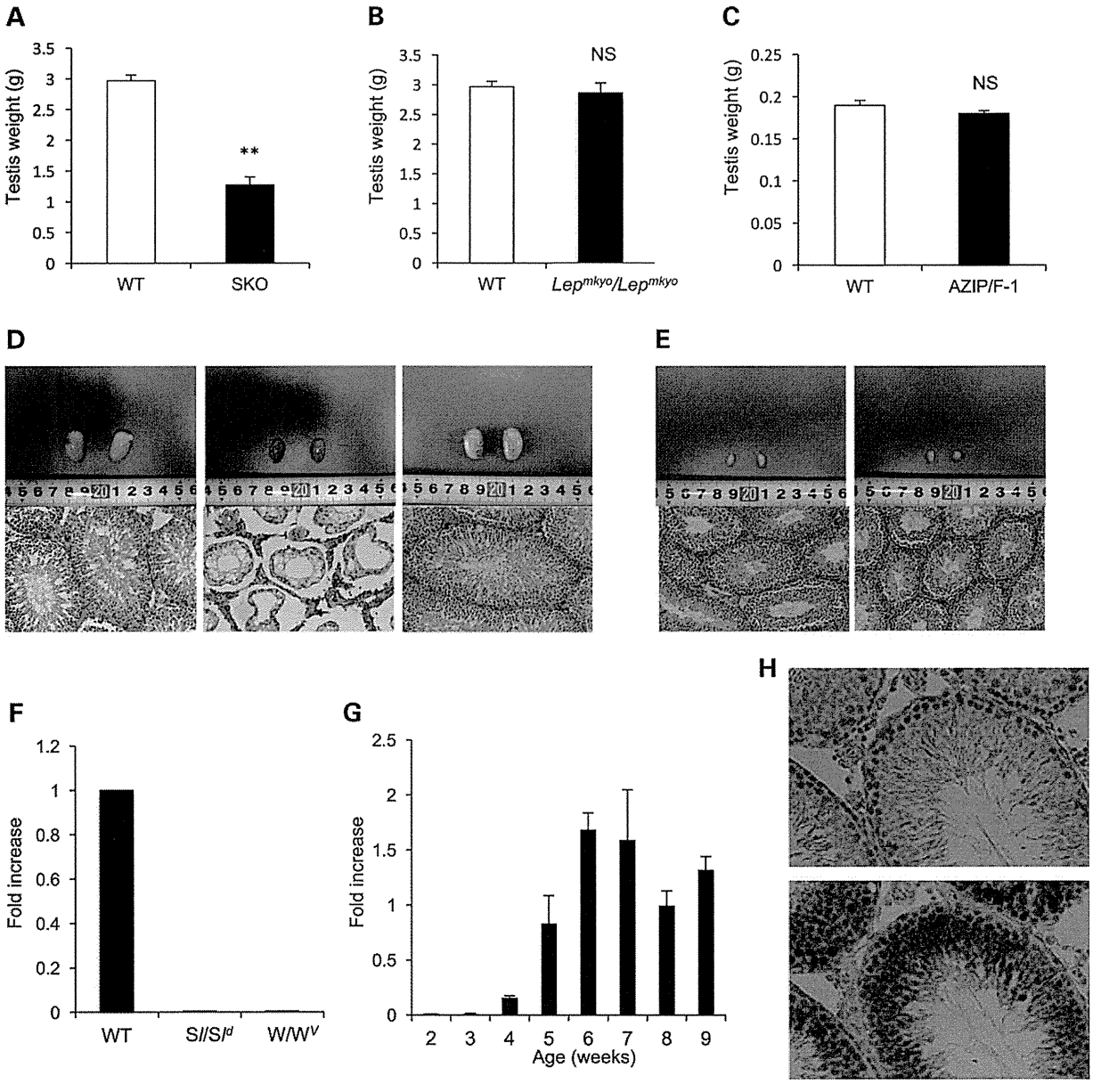

Figure 5. The role of seipin in the spermatogenesis. (A–C) Testis weight in SKO rats (A), *Lep*^{mkyo}/*Lep*^{mkyo} rats (B) and A-ZIP/F-1 mice (C). Values are mean ± SEM ($n = 10$ per group). **$P < 0.01$, NS, not significant (Student's *t*-test). (D and E) Macroscopic (top) and histological images (bottom) of the testis in WT (left), SKO (middle) and *Lep*^{mkyo}/*Lep*^{mkyo} (right) rats (D), and WT (left) and A-ZIP/F-1 (right) mice (E). For histological examination, hematoxylin and eosin staining was used. Original magnification of ×40 is shown. (F) *Bscl2* mRNA expressions checked with quantitative RT–PCR in the testis in 12-week-old WT, Sl/Sl^d and W/W^v mice. The fold change is displayed as relative to WT mice. $n = 6$ per group. (G) *Bscl2* mRNA expressions checked with quantitative RT–PCR in the testis during the period of postnatal development in WT rats. Values are mean ± SEM ($n = 6$ per group). (H) *Bscl2* expression pattern in the testis assessed by *in situ* hybridization in a WT rat. Images used with sense probe (top) and antisense probe (bottom) are shown. Original magnification of ×200 is shown.

concentrations including LH, FSH, testosterone and prolactin were within normal range in both patients (Supplementary Material, Table. S2). Although further study is needed, these results suggest the potential involvement of seipin in spermatogenesis in human.

Discussion

Using gene-driven ENU mutagenesis, we generated seipin deficient SKO rat. The mutation of *Bscl2* gene in SKO rats (*Bscl2*^{sko}) is located at nucleotide 239 in the third exon of *Bscl2*, generating a stop codon at amino acid 20 (L20X). Seipin has two distinct hydrophobic amino acid stretches and is speculated to have two transmembrane domains (1). L20X mutation is located upstream of these two transmembrane domains. In patients with lipodystrophy, nearly 30 *BSCL2* mutations have been reported so far (25). Among these *BSCL2* mutations, R275X mutation is the closest to the C-terminal (7). No relationship between the location of mutation site and severity of lipodystrophy is found, indicating that the region from the position at amino acid 275 to the C-terminal

Table 1. Semen examination in human BSCL2 patients

Variables	Patient 1	Patient 2	Cut-off value in WHO manual (2010)
Age	21	25	
Volume (ml)	3.6	1.5	1.5
Concentration (10^6/ml)	20	10	15
Total sperm number (10^6/ejaculate)	72	15	39
Motility (% motile)	75	60	40

is important for the physiological function of seipin. SKO rat that has a nonsense mutation located upstream of the two transmembrane domains is considered to have no functional seipin.

The mean mutation frequency with ENU mutagenesis of our protocol was one mutation per 3.7 million base pairs (20). Although the chance for the occurrence of an unexpected mutation with a phenotypic effect is relatively small, this possibility also should be taken account for the experimental design and interpretation of the results. To eliminate mutations that might have been generated by ENU in chromosomal regions other than the *Bscl2* locus, we performed backcross more than six generations against F344/NSlc inbred background, and we always compared phenotypes between littermates to minimize the effect of possible unexpected mutation.

The body weight in SKO rats was significantly lower than that in their WT littermates (Fig. 2A). Body composition analysis with computer tomography revealed that fat mass in both subcutaneous and intra-abdominal areas was markedly reduced while lean mass was obviously increased in SKO rats (Supplementary Material, Fig. S2A). In human patients with BSCL, organomegaly such as hepatosplenomegaly, cardiomegaly and muscular hypertrophy is generally observed as a consequence of hyperinsulinemia (17). We therefore compared weights in various tissues between SKO and WT rats and found that weights of the brain and the testis were significantly decreased in SKO rats in addition to the white and brown adipose tissues although weights of many other tissues were increased in SKO rats (Fig. 1F). Taking together with the fact that *Bscl2* mRNA is highly expressed in the brain and the testis (Fig. 1B), it was strongly suggested that seipin has an important role in the development of these two organs.

Patients with *BSCL2* mutation have the most severe variety of BSCL (13,25,26). They lack not only the 'metabolically active' adipose tissue such as subcutaneous and intra-abdominal ones but also the 'mechanical' adipose tissue located in the retro-orbital, bone marrow and so on (7,21). SKO rats lost more than 95% of fat mass in both subcutaneous and intra-abdominal areas (Supplementary Material, Fig. S2A), while more than 20% of fat mass in WT control mice was preserved in seipin knockout mice (14,15). We also confirmed no detectable adipose tissue in the bone marrow and retro-orbital areas in SKO rats by histological examination (Supplementary Material, Fig. S2E and F). On the other hand, even in BSCL2 patients, examination of subcutaneous biopsies found small adipocytes with low but detectable lipid content (27). In SKO rats, small adipocytes with small oil red O stained lipid droplets were also observed (Supplementary Material, Fig. S2D). SKO rat is a perfect model of human BSCL2 in terms of lipodystrophy and might be a useful model for the analysis of physiological roles of seipin in adipogenesis. We have already started the investigation with primary cultures of fibroblasts from SKO rats.

Lipodystrophy-associated phenotypes of SKO rats are also strikingly similar to those of human BSCL2 patients. Patients with severe lipodystrophy like BSCL2 generally exhibit insulin resistant but non-ketotic diabetes, hypertriglyceridemia, fatty liver, organomegaly and increased metabolic rate (17,26). While SKO rats had hyperglycemia with hyperinsulinemia (Fig. 3D), they did not have increased b-hydroxybutyrate level at baseline and fasting failed to increase it (Supplementary Material, Fig. S5E). Unlike *Bscl2* knockout mice (14–16), triglyceride level was markedly elevated in SKO rats (Fig. 3E). While it was reported that the expression of LDL-receptor in the liver was increased in *Bscl2* knockout mice (16), LDL-receptor mRNA expression was unchanged in SKO rats (data not shown). This might be the reason for the difference of triglyceride metabolism between mice and rats. Most organs except for adipose tissues, brain and testis were enlarged in SKO rats (Fig. 2B). Moreover, energy expenditure was increased in SKO rats as the oxygen consumption indicated (Supplementary Material, Fig. S1C). In contrast, *Bscl2* knockout mice showed a decrease in energy expenditure (16). The generation of SKO rat provided us a powerful tool for studying the pathophysiology of human BSCL2.

BSCL2 patients exhibit much higher rates of mild mental retardation than do patients with other BSCL genotypes (13). Although these cognitive defects were speculated to relate to the high expression of Bscl2 mRNA in the brain, it was also possible that the lack of adipose tissue contributes to the mental retardation. Furthermore, it had been reported that leptin secreted from adipocytes plays a role in the regulation of cognitive function (28,29). BSCL2 patients present with the most severe lipodystrophy and their leptin levels are extremely low. In this study, we evaluated the spatial working memory by Y-maze test not only in SKO rats but also leptin deficient Lep^{mkyo}/Lep^{mkyo} rats and A-ZIP/F-1 mice, a mouse model of generalized lipodystrophy and clearly revealed that the impairment of spatial working memory observed in SKO rats is due to neither leptin deficiency nor lipodystrophy (Fig. 3A–C). The spatial working memory of the rodents is responsible for recording information about the environment and the spatial orientation (30). In behavioral science, Y-maze is used to investigate how rodents function with spatial working memory from the early 20th century (31). This is the first report demonstrating that seipin deficiency itself leads to cognitive defect *in vivo*.

To identify the original region responsible for the impairment of spatial working memory in SKO rats, we examined the distribution of *Bscl2* mRNA expression in the whole brain by *in situ* hybridization in WT rats. *Bscl2* mRNA was ubiquitously expressed throughout the rostral–caudal extent of the rat brain including hippocampus, cerebellum, frontal and occipital cortex (Fig. 3D and E). Then, we compared the brain histologically between WT and SKO rats but we could not find any morphological changes throughout the brain (Fig. 3F). Next, we examined the neuron density in hippocampus, cerebellum and frontal cortex, there was no significant difference between WT and SKO rats in any layers or regions of these areas (Fig. 3G–I). These results and the fact that the whole brain volume was significantly reduced in SKO rats indicate that the total neuron number of the brain was decreased in SKO rats. No evidence of brain atrophy suggests that the cause of the reduction of neuron number is a suppression of neuron increment rather than a stimulation of neuron decrease such as apoptosis. Furthermore, no evidence of morphological abnormality suggests that the suppression of neuron increment might be due to disorder of neuron proliferation rather than disorder of neuron differentiation. The causal relationship between brain volume reduction and impairment of cognitive function in SKO rats is unclear since the present study did not deny the possibility

that seipin has a role in the neuronal function. In this study, we also found the reduction of brain volume in human BSCL2 patients although we need further study with more large number of patients to confirm it (Fig. 4A–C). Ventricular dilatation in CGL patients whose etiology was unknown was reported by pneumoencephalography (17). However, the ratio of subarachnoid area including cerebral ventricles to parenchymal area assessed by MRI in our patients showed no significant difference with that in healthy controls (Fig. 4C), demonstrating that our patients had no ventricular dilatation. In addition, while malformation of the hypothalamus in a CGL patient was also reported (32), all MRI images were assessed by radiologists and no morphological abnormality was pointed out in the present study. This is the first report indicating the pathophysiological role of seipin in the brain development in both rats and humans. Any apparent phenotypes of motor neuron disease that is associated with gain-of-toxic-function mutation in the N-glycosylation site of seipin (33) were not observed in both SKO rats and our BSCL2 patients.

SKO rats showed infertility with azoospermia. Testis weight was remarkably reduced and testis histology showed markedly shrunk spermatic duct and lack of mature sperm cells in SKO rats (Fig. 5D). These testis phenotypes were not observed in $Lep^{mkyo/Lepmkyo}$ rats and A-ZIP/F-1 mice, clearly indicating that the azoospermia observed in SKO rats is due to neither leptin deficiency nor lipodystrophy. Serum concentrations of gonadal hormones including LH, FSH and testosterone in SKO rats were all within normal range and were not significantly different from those in WT rats (Supplementary Material, Fig. S7). *Bscl2* mRNA is highly expressed in the testis. These facts indicate that the responsive region for the azoospermia in SKO rats is the testis itself. Analyses using with Sl/Sl^d and W/W^v mice demonstrated that *Bscl2* mRNA is expressed in neither Sertoli nor Spermatogonia cells. In addition, the analysis during the period of postnatal development in WT rats demonstrated that the significant increment of *Bscl2* mRNA expression was detected only from 5 to 6 weeks. WT rat produces mature sperm cells from the age of 6 or 7 weeks old. Consistent with these results, analysis of WT rat testis by *in situ* hybridization showed that *Bscl2* mRNA was not expressed in spermatogonia cells. These results indicate that seipin has an important role in the late phase of spermatogenesis in rats.

At least one male BSCL2 patient has been reported with multiple healthy children (17,25). However, semen examination in this patient was not reported. Recently, one other male BSCL2 patient was reported to have teratozoospermia (19). There was also no information on the number of sperm in this patient. In this study, we performed semen examination in two BSCL2 male patients and found that one patient had oligospermia according to the WHO criteria and the other had low sperm concentration but above the cut-off value of the criteria. Although further study is required, these results suggest the potential involvement of seipin in spermatogenesis in human.

In conclusion, through the generation and analysis of SKO rat, a rat model of BSCL2, we found that seipin deficiency leads to impairment of cognitive function with brain weight reduction and infertility with azoospermia in addition to generalized lipodystrophy, those have not been reported in seipin KO mice. We also confirmed reduction of brain volume and number of sperm in human patients with *BSCL2* mutation although further study is needed to clarify human phenotypes. This is the first report demonstrating that seipin is necessary for normal brain development and spermatogenesis in addition to white adipose tissue development.

Materials and Methods

Animals

Rats with a *Bscl2* mutation were obtained by ENU mutagenesis of F344/NSlc rats, followed by MuT-POWER (Mu Transposition POoling method With sequencER) screening on the genomic DNA of 4608 G1 male offspring in KURMA (Kyoto University Rat Mutant Archive). ENU mutagenesis procedures, screening protocols (20) and intracytoplasmic sperm injection procedure were previously described (34) The forward primer and the reverse primer used for identifying mutation of *Bscl2* were 5′-GATGTTGCTTTGT CCTGCTA-3′ and 5′-TTTCTCGGTTTTTCACCAC-3′, respectively. More than six backcross generations were performed against the F344/NSlc inbred background. Genotyping for $Bscl2^{sko}$mutation was performed by real-time PCR system using TaqMan Sample-to-SNP kit (Applied Biosystems, Carlsbad, CA, USA) with a specific primer pair (Forward primer sequences are 5′-TGTGGG CCCAGGAAGTG-3′ and reverse primer sequences are 5′-CCCCA AACTGCAGCATCAG-3′) and TaqMan MGB probes (WT probe sequences are 5′-CCTGCCTACACATGG-3′ and mutant probe sequences are 5′-CCTGCCAACACATGG-3′). Genomic DNA was extracted from whole blood. The cycling conditions were 20 s at 95°C followed by 40 cycles of 3 s at 95°C and 20 s at 60°C. F344/NSlc rats and C57Bl/6J mice were purchased (Japan SLC, Hamamatsu, Japan). Lep^{mkyo}/ Lep^{mkyo} rats on F344/NSlc background were generated previously (35). A-ZIP/F-1 mice were provided from Diabetes Branch, National Institute of Diabetes and Digestive and Kidney Diseases (Bethesda, MD, USA) (22). Sl/Sl^d mice and W/W^v mice were purchased from Japan SLC. Rats and mice were maintained on a 14 h light/10 h dark cycle (lights on 7:00 AM, lights off 9:00 PM) and fed ad libitum standard pellet diet (MF; Oriental Yeast, Tokyo, Japan).

All animal care and experiments conformed to the Guidelines for Animal Experiments at Kyoto University and were approved by the Animal Research Committee of Kyoto University.

Real-time quantitative RT–PCR for Bscl2 mRNA expression

Each tissue was frozen in liquid nitrogen and stored at −80°C until use for RNA isolation. RNA was prepared using Trizol (Invitrogen, Carlsbad, CA, USA) reagent following the supplier's protocol. The Quality and the concentrations of the extracted RNA were checked using the Nano-Drop 2000 (Thermo Scientific, Yokohama, Japan). Single-stranded cDNA was synthesized from 1 μg of total RNA using SuperScript III First-Strand Synthesis System for RT–PCR, according to the manufacturer's instructions (Invitrogen). Quantitative RT–PCR was performed with SYBR Green (Applied Biosystems) by Applied Biosystems StepOnePlus™ RT–PCR System using gene specific primer. The housekeeping rat or mouse mitochondrial subunit 18S rRNA genes were used for control and quantitative RT–PCR was performed with TaqMan (Applied Biosystems). The sequences of primers (Sigma-Genosys, Tokyo, Japan) used in the present study are as follows: rat *Bscl2* forward; 5′-CCCACAAGTGATTTGAGTTGGGGA-3′, rat *Bscl2* reverse; 5′-GTGGGTGACGGTCGGCATGT-3′, mouse *Bscl2* forward; 5′-GGTTCT CGCCGCTTACGTTGCG-3′, mouse *Bscl2* reverse; 5′-GGTCTCCCAGC TCGCGTCACT-3′, rat 18s forward; 5′-GCAATTATTCCCCATGAAC GA-3′, rat 18s reverse; 5′-CAAAGGGCAGGGACTTAATCAAC-3′, probe; 5′-AATTCCCAGTAAGTGCGGGTCATAAGCTTG-3′, mouse 18s forward; 5′-CGCGCAAATTACCCACTCCCGA-3′, mouse 18s reverse; 5′-CGGCTACCACATCCAAGGA-3′, probe; 5′-CCAATTA CAGGGCCTCGAAA-3′.

Computed tomography

Computed tomography (CT) image of 20-week-old male rats was obtained under anesthesia by La Theta LCT-100 (Aloka, Tokyo, Japan).

Biochemical assays

Blood was obtained from the tail vein under ad libitum feeding at the age of 20 weeks if not otherwise specified. Plasma leptin concentrations were measured by an enzyme-linked immunosorbent assay (ELISA) kit for rat leptin (Millipore, St Charles, MO, USA). Plasma glucose concentrations were measured by a glucose assay kit (Wako Pure Chemical Industries, Osaka, Japan). Plasma insulin concentrations were measured by an insulin-ELISA kit (Morinaga Institute of Biological Science, Yokohama, Japan). Plasma triglyceride concentrations were measured by an enzymatic kit (Triglyceride E-test Wako; Wako Pure Chemical Industries).

Glucose tolerance test

Intraperitoneal glucose tolerance test (IPGTT) was performed after overnight fasting in 20-week-old male rats. Rats received 2.0 mg/g glucose by intraperitoneal injection. Blood was sampled from the tail vein before and 15, 30, 60, 90, 120 min after the glucose load.

Histology

Rat livers and rat and mouse testes were fixed in 10% neutrally buffered formalin and subsequently embedded in paraffin. Histological sections of 5 mm thickness were stained with hematoxylin and eosin. Rat brains were sampled after perfusion with 4% paraformaldehyde under anesthesia by intraperitoneal injection of sodium pentobarbital (DS Pharma Biomedical, Suita, Japan), fixed in 4% paraformaldehyde and subsequently embedded in paraffin. Sagital sections of 4 mm thickness were Nissl stained with 0.1% Cresyl violet solution.

Y-maze test

Spatial working memory was assessed by the Y-maze test in 20-week-old male SKO rats, Lep^{mkyo}/ Lep^{mkyo} rats and A-ZIP/F-1 mice as described previously (36). Briefly, the Y-maze test was conducted during the dark period (9:00 PM to 11:00 PM) in a dimly illuminated room. The maze consists of three arms (for rats; 425 mm long, 225 mm high and 145 mm wide, for mice; 300 mm long, 150 mm high and 60 mm wide, labeled A, B or C) diverging at a 120° from the central point. Each rat was placed at the end of the start arm and allowed to move freely through the maze during an 8-min session. The sequence of arm entries was manually recorded. An actual alternation was defined as entries into all the three arms on consecutive occasions. The maximum alternation was subsequently calculated by measuring the total number of arm entries minus 2 and the percentage of alternation was calculated as (actual alternations/maximum alternations) ×100. The total number of arms entered during the sessions, which reflect locomotor activities, was also recorded.

In situ hybridization of Bscl2 mRNA

In situ hybridization was performed as described previously (37). Briefly, to prepare cRNA probes, cDNA fragments encoding rat *Bscl2* (NM_001012171.1 sequence166–1092) was amplified. Digoxigenin-labeled sense and antisense probes were synthesized with RNA polymerases. To obtain paraffin-embedded blocks and sections of rat brain and testis, rats were dissected after its perfusion. Rat brains and testes were fixed in 4% paraformaldehyde and embedded in paraffin. Sections of 6 mm thickness were deparaffinized, fixed, hydrogen chloride treated. Hybridization was performed with antisense or sense probe (100 ng/ml) at 60°C for 16 h in hybridization solution (Genostaff, Tokyo, Japan). Hybrids were detected with anti-DIG alkaline phosphate-conjugated antibody (Roche Diagnostics GmbH, Basal, Switzerland) and coloring reactions were performed with NBT/BCIP solution (Sigma-Aldrich Japan, Tokyo, Japan). The sections were counterstained with Kernechtrot stain solution (Muto Pure Chemicals, Tokyo, Japan).

Analysis of cell number in the brain sections

Four regions (CA1, CA2, CA3, DG) of hippocampus and five layers (I, II+III, IX, V, VI) of frontal cortex were photographed at high magnification (×400), respectively (Supplementary Material, Fig. S6A and C). The number of Nissl stained cells in a photographed visual field (0.275 × 0.4125 mm) was counted. The molecular cell layer and granular cell layer of cerebellum were also photographed at high magnification (×400), but the number of stained cells was counted in a smaller visual field (0.13 × 0.4125 mm) (Supplementary Material, Fig. S6B). Purkinje cell layer of cerebellum is a monolayer and the number of stained cells in this layer was just counted in a photograph at high magnification (×400) (Supplementary Material, Fig. S6B).

Measurement of brain size in BSCL2 patients

Brain size of BSCL2 patients was assessed by MRI technique. Whole brain images were acquired by a 3-Tesla Trio MRI scanner (Siemens, Erlangen, Germany) in axial orientation using the following parameters: repetition time, 3000 ms; echo time, 30 ms; flip angle, 90°; voxel size, 3 × 3 × 3 mm; field of view, 192 × 192 mm; matrix size, 64 × 64; and number of slices, 48 (38). Whole brain volume was calculated with the Virtual Place software (AZE, Tokyo, Japan). Brain parenchymal and subarachnoid areas of three different coronal sections, those are just above the bilateral ventricles, in center of the lateral ventricles and through interventricular foramen, were calculated by Image J software (NIH, Bethesda, MD, USA). Study protocols were approved by the Ethical Committee of Kyoto University Graduate School of Medicine. After detailed explanation of the study design, written informed consent was obtained from all subjects before study initiation.

Semen examination in BSCL2 patients

Semen examination was performed in two young adult male BSCL2 patients. One was 24 years old with E189X homozygous mutation and the other was 28 years old with R275X homozygous mutation in *BSCL2* gene. Semen samples were collected by masturbation that followed 3 days of sexual abstinence. Ejaculate volume and concentration of spermatozoa and percentage of motile spermatozoa in semen were analyzed at room temperature immediately after complete liquefaction (2 h). Motility was determined by Cellsoft Automated Semen Analyzer (Cryo Resources, New York, NY, USA).

Statistical analysis

Data are expressed as means ± SEM. Comparison between or among groups was assessed by Student's *t* test or ANOVA with

Fisher's protected least significant difference test. χ^2 test was used for analysis of Mendelian ratios of genotype and sex. $P < 0.05$ was considered statistically significant.

Supplementary Material

Supplementary Material is available at *HMG* online.

Acknowledgements

We thank Takashi Shinohara for discussion and Keiko Hayashi for technical assistance. The authors also acknowledge Yoko Koyama for secretarial assistance.

Conflict of Interest statement. None declared.

Funding

This work was supported by research grants from the Japanese Ministry of Education, Culture, Sports, Science and Technology, the Japanese Ministry of Health, Labor and Welfare, Uehara Memorial Foundation, The European Community's Seventh Framework Programme (FP7/2007–2013) under grant agreement no. HEALTH-F4-2010-241504 (EURATRANS) and Industrial Technology Research Grant Program from New Energy and the Industrial Technology Development Organization (NEDO) of Japan.

References

1. Magré, J., Delépine, M., Khallouf, E., Gedde-Dahl, T. Jr, Van Maldergem, L., Sobel, E., Papp, J., Meier, M., Mégarbané, A., Bachy, A. *et al.* (2001) Identification of the gene altered in Berardinelli-Seip congenital lipodystrophy on chromosome 11q13. *Nat. Genet.*, **28**, 365–370.
2. Capeau, J., Magré, M., Caron-Debarle, M., Lagathu, C., Antoine, B., Bérériat, V., Lascols, O. and Bastard, J.P. (2010) Human lipodystrophies: genetic and acquired diseases of adipose tissue. *Endocr. Dev.*, **19**, 1–20.
3. Garg, A. (2011) Lipodystrophies: genetic and acquired body fat disorders. *J. Clin. Endocrinol. Metab.*, **96**, 3313–3325.
4. Agarwal, A.K., Arioglu, E., De Almeida, S., Akkoc, N., Taylor, S. L., Bowcock, A.M. and Garg, A. (2002) AGPAT2 is mutated in congenital generalized lipodystrophy linked chromosome 9q34. *Nat. Genet.*, **31**, 21–23.
5. Kim, C.A., Delépine, M., Boutet, E., El Mourabit, H., Le Lay, S., Meier, M., Nemani, M., Bridel, E., Leite, C.C., Bertola, D.R. *et al.* (2008) Association of a homozygous nonsense caveolin-1 mutation with Berardinelli-Seip congenital lipodystrophy. *J. Clin. Endocrinol. Metab.*, **93**, 1129–1134.
6. Hayashi, Y.K., Matsuda, C., Ogawa, M., Goto, K., Tominaga, K., Mitsuhashi, S., Park, Y.E., Nonaka, I., Hino-Fukuyo, N., Haginoya, K. *et al.* (2009) Human PTRF mutations cause secondary deficiency of caveolins resulting in muscular dystrophy with generalized lipodystrophy. *J. Clin. Invest.*, **119**, 2623–2633.
7. Ebihara, K., Kusakabe, T., Masuzaki, H., Kobayashi, N., Tanaka, T., Chusho, H., Miyanaga, F., Miyazawa, T., Hayashi, T., Hosoda, K. *et al.* (2004) Gene and phenotype analysis of congenital generalized lipodystrophy in Japanese: a novel homozygous nonsense mutation in seipin gene. *J. Clin. Endocrinol. Metab.*, **89**, 2360–2364.
8. Agarwal, A.K. and Garg, A. (2003) Congenital generalized lipodystrophy: significance of triglyceride biosynthetic pathways. *Trends. Endocrinol. Metab.*, **14**, 214–221.
9. Garg, A. and Agarwal, A.K. (2008) Caveolin-1: a new locus for human lipodystrophy. *J. Clin. Endocrinol. Metab.*, **93**, 1183–1185.
10. Windpassinger, C., Auer-Grumbach, M., Irobi, J., Patel, H., Petek, E., Hörl, G., Malli, R., Reed, J.A., Dierick, I., Verpoorten, N. *et al.* (2004) Heterozygous missense mutations in BSCL2 are associated with distal hereditary motor neuropathy and Silver syndrome. *Nat. Genet.*, **36**, 271–276.
11. Chen, W., Yechoor, V.K., Chang, B.H., Li, M.V., March, K.L. and Chan, L. (2009) The human lipodystrophy gene product Berardinelli-Seip congenital lipodystrophy 2/seipin plays a key role in adipocyte differentiation. *Endocrinology*, **150**, 4552–4561.
12. Ito, D. and Suzuki, N. (2007) Molecular pathogenesis of seipin/BSCL2-related motor neuron diseases. *Ann. Neurol.*, **61**, 237–250.
13. Maldergem, V.L., Magré, J., Khallouf, T.E., Gedde-Dahl, T. Jr, Delépine, M., Trygstad, O., Seemanova, E., Stephenson, T., Albott, C.S. and Bonnici, F. (2002) Genotype-phenotype relationships in Berardinelli-Seip congenital lipodystrophy. *J. Med. Genet.*, **39**, 722–733.
14. Cui, X., Wang, Y., Tang, Y., Liu, Y., Zhao, L., Deng, J., Xu, G., Peng, X., Ju, S., Liu, G. and Yang, H. (2011) Seipin ablation in mice results in severe generalized lipodystrophy. *Hum. Mol. Genet.*, **20**, 3022–3030.
15. Chen, W., Chang, B., Saha, P., Hartig, S.M., Li, L., Reddy, V.T., Yang, Y., Yechoor, V., Mancini, M.A. and Chan, L. (2012) Berardinelli–Seip congenital lipodystrophy 2/seipin is a cell-autonomous regulator of lipolysis essential for adipocyte differentiation. *Mol. Cell Biol.*, **32**, 1099–1111.
16. Prieur, X., Dollet, L., Takahashi, M., Nemani, M., Pillot, B., Le May, C., Mounier, C., Takigawa-Imamura, H., Zelenika, D., Matsuda, F. *et al.* (2013) Thiazolidinediones partially reverse the metabolic disturbances observed in Bscl2/seipin-deficient mice. *Diabetologia*, **56**, 1813–1825.
17. Seip, M. and Trygstad, O. (1996) Generalized lipodystrophy, congenital and acquired (lipoatrophy). Acta Paediatr. Suppl., **413**, 2–28.
18. Zhou, L., Yin, J., Wang, C., Liao, J., Liu, G. and Chen, L. (2014) Lack of seipin in neurons results in anxiety- and depression-like behaviors via down regulation of PPARγ. *Hum. Mol. Genet.*, **15**, 4094–4102.
19. Jiang, M., Mingming, G., Chaoming, W., Hui, H., Kuejiang, G., Zuomin, Z., Hongyuan, Y., Kinhua, X., George, L. and Jiahao, S. (2014) Lack of testicular seipin causes teratozoospermia in men. *Proc. Natl Acad. Sci. USA*, **111**, 7054–7059.
20. Mashimo, T., Yanagihara, K., Tokuda, S., Voigt, B., Takizawa, A., Nakajima, R., Kato, M., Hirabayashi, M., Kuramoto, T. and Serikawa, T. (2008) An ENU-induced mutant archive for gene targeting in rats. *Nat. Genet.*, **40**, 514–515.
21. Simha, V. and Garg, A. (2003) Phenotypic heterogeneity in body fat distribution in patients with congenital generalized lipodystrophy caused by mutations in the AGPAT2 or seipin genes. *J. Clin. Endocrinol. Metab.*, **88**, 5433–5437.
22. Moitra, J., Mason, M.M., Olive, M., Krylov, D., Gavrilova, O., Marcus-Samuels, B., Feigenbaum, L., Lee, E., Aoyama, T., Eckhaus, M. *et al.* (1998) Life without white fat: a transgenic mouse. *Genes. Dev.*, **12**, 3168–3181.
23. Tadokoro, Y., Tomogida, K., Ohta, H., Tohda, A. and Nishiume, Y. (2002) Homeostatic regulation of germinal stem cell proliferation by the GDNF/FSH pathway. *Mech. Dev.*, **113**, 29–39.
24. Ohta, H., Yomogida, K., Dohmae, K. and Nishuume, Y. (2000) Regulation of proliferation and differntiation in spermatogonial cells: the role of c-kit and its ligand SCF. *Development*, **127**, 2125–2131.

25. Cartwright, B.R. and Goodman, J.M. (2012) Seipin: from human disease to molecular mechanism. *J. Lipid. Res.*, **53**, 1042–1055.
26. Garg, A. (2004) Acquired and inherited lipodystrophies. *N. Engl. J. Med.*, **350**, 1220–1234.
27. Rogunum, T.O., Bjerve, K.S., Seip, M., Trygstad, O. and Oseid, S. (1978) Fat cell size and lipid content of subcutaneous tissue in congenital generalized lipodystrophy. *Acta Endocrinol.*, **88**, 182–189.
28. Harvey, J. (2007) Leptin regulation of neuronal excitability and cognitive function. *Curr. Opin. Pharmacol.*, **7**, 643–647.
29. Morrison, C.D. (2009) Leptin signaling in brain: a link between nutrition and cognition? *Biochim. Biophys. Acta*, **1792**, 401–408.
30. O'Keefe, J. and Dostrovsky, J. (1971) The hippocampus as a spatial map. Preliminary evidence from unit activity in the freely-moving rat. *Brain Res.*, **34**, 171–175.
31. Olton, D.S. (1976) Mazes, maps, and memory. *Am. Psychol.*, **34**, 583–596.
32. Berge, T., Brun, A., Hansing, B. and Kjellman, B. (1976) Congenital generalized lipodystrophy. *Acta Pathol. Microbiol. Scand. A.*, **86**, 47–54.
33. Ito, D. and Suzuki, N. (2009) Seipinopathy: a novel endoplasmic reticulum stress-associated disease. *Brain*, **132**, 8–15.
34. Hirabayashi, M., Kato, M., Aoto, T., Ueda, M. and Hochi, S. (2002) Rescue of infertile transgenic rat lines by intracytoplasmic injection of cryopreserved round spermatids. *Mol. Reprod. Dev.*, **62**, 295–299.
35. Aizawa-Abe, M., Ebihara, K., Ebihara, C., Mashimo, T., Takizawa, A., Tomita, T., Kusakabe, T., Yamamoto, Y., Aotani, D., Yamamoto-Kataoka, S. *et al.* (2013) Generation of leptin-deficient Lepmkyo/Lepmkyo rats and identification of leptin-responsive genes in the liver. *Physiol. Genomics.*, **45**, 786–793.
36. Kitamura, A., Fujita, Y., Oishi, N., Kalaria, R.N., Washida, K., Maki, T., Okamoto, Y., Hase, Y., Yamada, M., Takahashi, J. *et al.* (2012) Selective white matter abnormalities in a novel rat model of vascular dementia. *Neurobiol. Aging*, **33**, 25–35.
37. Koizumi, A., Shigemoto-Mogami, Y., Nasu-Tada, K., Shinozaki, Y., Ohsawa, K., Tsuda, M., Joshi, B.V., Jacobson, K.A., Kohsaka, S. and Inoue, K. (2007) Floral development of an asexual and female-like mutant carrying two deletions in gynoecium-suppressing and stamen-promoting functional regions on the Y chromosome of the dioecious plant Silene latifolia. *Plant. Cell Physiol.*, **48**, 1450–1461.
38. Aotani, D., Ebihara, K., Sawamoto, N., Kusakabe, T., Aizawa-Abe, M., Kataoka, S., Sakai, T., Iogawa, H., Ebihara, C., Fujikura, J. *et al.* (2012) Functional magnetic resonance imaging analysis of food-related brain activity in patients with lipodystrophy undergoing leptin replacement therapy. *J. Clin. Endocrinol. Metab.*, **97**, 3663–3671.

厚生労働科学研究費補助金（創薬基盤推進研究事業）
新規創薬を目指した生活習慣病・難治性疾患モデル遺伝子変異ラットの開発と解析
平成２４年度～２６年度　総合研究報告書

発行者　厚生労働科学研究費補助金（創薬基盤推進研究事業）
新規創薬を目指した生活習慣病・難治性疾患モデル遺伝子変異ラットの開発と解析
研究代表者　　中尾　一和

連絡先：〒606-8507　京都市左京区聖護院川原町
京都大学大学院医学研究科
メディカルイノベーションセンター
TEL：075-366-7450